

# UBE2T promotes epithelial-mesenchymal transition and motility in oral cancer cells via induction of IL-6 expression

AI WATANABE $^{1,2*}$ , JIN LU $^{2*}$ , KAI ISHIHARA $^{2,3}$ , SADAHIRO IWABUCHI $^{4,6}$ , KAZUCHIKA OHNO $^1$ , SHINICHI HASHIMOTO $^4$ , TAKAHIRO ASAKAGE $^1$ , KAZUKI TAKAHASHI $^2$ , KATARZYNA A. PODYMA-INOUE $^2$  and TETSURO WATABE $^{2,5}$ 

Department of Head and Neck Surgery, Graduate School of Medical and Dental Sciences, Institute of Science Tokyo,
 Tokyo 113-8510, Japan; Department of Biochemistry, Graduate School of Medical and Dental Sciences, Institute of Science Tokyo,
 Tokyo 113-8510, Japan; Department of Maxillofacial Surgery, Graduate School of Medical and Dental Sciences,
 Institute of Science Tokyo, Tokyo 113-8510, Japan; Department of Molecular Pathophysiology, Wakayama Medical University,
 Wakayama 641-8509, Japan; Soral Science Center, Institute of Biomedical Engineering, Institute of Science Tokyo, Tokyo 113-8510, Japan

Received March 26, 2025; Accepted July 17, 2025

DOI: 10.3892/ol.2025.15219

**Abstract.** Oral squamous cell carcinoma (OSCC) is a prevalent aggressive malignancy with a high mortality rate. However, the mechanisms underlying the progression of OSCC remain to be elucidated. In the present study, bioinformatics analysis

Correspondence to: Dr Katarzyna A. Podyma-Inoue or Dr Tetsuro Watabe, Department of Biochemistry, Graduate School of Medical and Dental Sciences, Institute of Science Tokyo, 1-5-45 Yushima, Bunkyo, Tokyo 113-8510, Japan

E-mail: kapobch@tmd.ac.jp E-mail: t-watabe.bch@tmd.ac.jp

Present address: <sup>6</sup>Department of Bioinformatics and Genomics, Graduate School of Advanced Preventive Medical Sciences, Kanazawa University, Kanazawa, Ishikawa 920-8641, Japan

# \*Contributed equally

Abbreviations: ANKRD1, ankyrin repeat domain 1; DEGs, differentially expressed genes; DMEM, Dulbecco's modified Eagle's medium; EMT, epithelial-mesenchymal transition; FBS, fetal bovine serum; GEPIA, gene expression profiling interactive analysis; GO, Gene Ontology; GSEA, gene set enrichment analysis; HNSCC, head and neck squamous cell carcinoma; IL-6, interleukin-6; JAK, Janus protein tyrosine kinase; KM-plotter, Kaplan-Meier plotter; MET, mesenchymal-epithelial transition; MMP-9, matrix metalloproteinase-9; NES, normalized enrichment score; OSCC, oral squamous cell carcinoma; PI3K, phosphatidylinositol 3-kinase; PLAU, plasminogen activator, urokinase; RT-qPCR, reverse transcription-quantitative PCR; STAT3, signal transducer and activator of transcription 3; STRING, Search Tool for the Retrieval of Interacting Genes/Proteins; TGF-β, transforming growth factor-β; TME, tumor microenvironment; TPM, transcripts per million; UBE2T, ubiquitin-conjugating enzyme E2 T

Key words: OSCC, UBE2T, EMT, IL-6

identified ubiquitin-conjugating enzyme E2 T (UBE2T) as a poor prognostic factor in head and neck cancer, showing the strongest association with cancer stage progression. Functional studies revealed that UBE2T can enhance motility and induce epithelial-mesenchymal transition (EMT) in OSCC cells. RNA sequencing and subsequent analyses demonstrated that UBE2T upregulated the expression levels of various motility- and EMT-related factors, including ankyrin repeat domain 1, endothelin-1, interleukin-6 (IL-6), matrix metalloproteinase-9 and plasminogen activator, urokinase. Gene set enrichment analysis indicated that UBE2T activates the IL-6/Janus protein tyrosine kinase (JAK)/signal transducer and activator of transcription 3 signaling pathway. Moreover, treatment of OSCC cells with IL-6 or a JAK inhibitor resulted in the induction of EMT and mesenchymal-epithelial transition, respectively, accompanied by enhanced and suppressed cancer cell motility. These results indicated that IL-6, which is upregulated by UBE2T, may be crucial for maintaining mesenchymal traits and motility in OSCC cells. Collectively, these findings suggested that the UBE2T/IL-6/JAK axis may serve as a potential therapeutic target for OSCC.

#### Introduction

Metastasis is the primary cause of cancer-related death. It is regulated by complex molecular mechanisms that enhance cancer cell motility and invasiveness (1) and involves multiple steps, including local invasion, intravasation, survival in circulation, extravasation, and colonization at the distant sites (2). Transforming growth factor-β (TGF-β), Wnt/β-catenin, and mitogen-activated protein kinase cascades are the key signaling pathways that facilitate these metastatic events (1-4). The tumor microenvironment (TME) significantly influences cancer development and metastasis by interacting with various cellular components of the extracellular matrix. Genetic and epigenetic modifications within tumor cells and components of the TME drive changes in cancer cell characteristics, leading to the alteration of genes participating in the metastatic

process (5). These changes can result in enhanced cancer cell migration and proliferation, effective extracellular matrix remodeling, or tumor vessel formation (2). Therefore, understanding mechanisms controlling these events is essential for the development of effective strategies to suppress cancer metastasis (2).

Oral cancer is a significant global health concern with increasing prevalence and mortality rates (6-8). In 2022, 389,846 new cases and 188,438 deaths due to cancers of the lip and oral cavity were reported, representing a significant increase from previous years (6,7,9). Oral squamous cell carcinoma (OSCC) is the most common type of oral cancer, accounting for over 90% of oral cancer cases, and is characterized by a high incidence and aggressiveness (10). Epithelial-mesenchymal transition (EMT) plays crucial roles in OSCC progression, metastasis, and drug resistance (11). During the EMT, OSCC cells lose their epithelial characteristics and gain mesenchymal properties, thereby increasing their aggressiveness and motility (12). This process involves a decrease in the expression of the epithelial cell marker E-cadherin, accompanied by an increased expression of the mesenchymal cell marker vimentin (12). EMT endows cancer cells with migratory, invasive, and stem-like properties, contributing to local recurrence and lymph node metastasis; thus, its targeting is crucial for the development of effective OSCC treatments. Several signaling pathways, including TGF-β, and Wnt/β-catenin are involved in EMT regulation in OSCC (11). To prevent OSCC progression and improve patient outcomes, it is important to understand the molecular mechanisms underlying EMT and identify factors whose expression is upregulated during the onset and progression of OSCC, leading to the induction of EMT.

Cancer progression is also regulated by factors that regulate the dynamics of the TME (1). Recent lines of evidence suggest that ubiquitin-proteasome pathways play crucial roles in the modulation of cancer-associated pathways (13). Ubiquitination has been implicated in autophagy (14) or ferroptosis (15) affecting cell growth and apoptosis (16). A recent report has revealed that the dysregulation of ubiquitination pathways might lead to enhanced cancer cell growth and metastasis (17). Among the members of the ubiquitin-proteasome family, ubiquitin-conjugating enzyme E2 T (UBE2T) has emerged as an important factor in the progression of multiple types of cancer (18,19). Upregulated UBE2T expression is known to induce EMT in multiple types of tumors, by activating the Wnt/β-catenin pathway (20,21), Akt/glycogen synthase kinase-3  $\beta/\beta$ -catenin pathway, or phosphatidylinositol 3-kinase (PI3K)/Akt pathway (22). However, little is known about the role of increased UBE2T expression and the factors regulated by UBE2T during OSCC progression.

In this study, we aimed to identify factors that play critical roles in the progression and tumorigenic potential of oral cancer cells. By elucidating the molecular mechanisms underlying the EMT, we hope to contribute to the development of innovative therapeutic strategies for the treatment of oral cancer.

## Materials and methods

Reagents. Recombinant human interleukin-6 (IL-6) was purchased from R&D and was reconstituted in Dulbecco's

phosphate-buffered saline. IL-6 was used at concentration of 10 ng/ml in cell culture experiments as described in later section. A Janus protein tyrosine kinase (JAK) inhibitor, ruxolitinib (23,24), was obtained from Seleck and used at the concentration of 1  $\mu$ M.

Cell culture. Human OSCC cell line; SAS was obtained from RIKEN BioResource Center Cell Bank (RCB1974; RRID:CVCL1675). The SAS cells with fluorescent ubiquitination-based cell cycle indicators (Fucci), termed 'SAS-Fucci', were established as previously described (25) by introducing Fucci plasmids (CFII-EF mKO2-hCdt1 [30/120] and CFII-EF-mAG-hGeminin [1/110]), a kind gift from Dr. Atsushi Miyawaki (26). SAS-Fucci cells were maintained in Dulbecco's Modified Eagle's Medium (DMEM; Nacalai Tesque) supplemented with 10% fetal bovine serum (FBS; Sigma or Biowest), 100 units/ml penicillin, and 100  $\mu$ g/ ml streptomycin (Nacalai Tesque) in a humidified incubator at 37°C with 5% CO<sub>2</sub>. 293FT (Thermo Fisher Scientific, R70007; RRID:CVCL6911) were maintained in DMEM supplemented with 10% FBS, 1% non-essential amino acid solution (Nacalai Tesque), 100 units/ml penicillin, and 100 µg/ ml streptomycin in a humidified incubator at 37°C with 5%

Depending on the experiment, cells were treated either with IL-6 or ruxolitinib and subjected to reverse transcription-quantitative PCR (RT-qPCR) or cell migration assay as described in later sections,

Identification of factors critical for the progression of head and neck cancer. Gene Expression Profiling Interactive Analysis (GEPIA; http://gepia.cancer-pku.cn/ index.html) (27), a web server for assessing RNA expression data from The Cancer Genome Atlas along with the 'Genotype-Tissue Expression' projects, was used to investigate the top 500 genes of enhanced expression in head and neck squamous cell carcinoma (HNSCC) database. Expressions of candidate genes in HNSCC tumors vs. their expressions in normal tissues were assessed using differential gene expression analysis with GEPIA web server. The significance was estimated with utility in GEPIA employing one-way ANOVA, using disease state (Tumor or Normal) as variable for calculating differential expression. The correlation between gene expression and stage progression of HNSCC was investigated using 'Stage Plot' utility within GEPIA. The pathological stage was considered as variable for calculating differential expression; 'gene expression ~ pathological stage'. Significance of differential gene expression between stages was estimated using one-way ANOVA. For differential analysis the expression data presented in transcripts per million (TPM) values were log<sub>2</sub> transformed after adding 1 followed by log<sub>2</sub>FC defined as median(Tumor)-median(Normal).

Kaplan-Meier plotter (KM-plotter) analysis. Survival of patients HNSCC was determined using KM-plotter (https://kmplot.com/analysis/) (28). Overall survival of patients was assessed for 500 candidate genes splitting patients at 'auto best select cut-off'. This analysis was based on the RNA sequence dataset of 500 patients with HNSCC available in the



KM-plotter. The P-value was computed with utility available in the KM-plotter using the Cox-Mantel (log rank) test.

Construction of plasmid DNA. The experimental procedures were approved by Genetically Modified Organisms Safety Committee of Institute of Science Tokyo (approval numbers: G2019-026C9 and G2024-007C5). Human UBE2T cDNA (GenBank Accession No. NM 001310326.2) was amplified using KOD Plus Neo DNA polymerase (TOYOBO) with gene specific primers. The forward primer contained a BamHI restriction site and Kozak sequence, while the reverse primer contained an XhoI restriction site. The sequences of the primers are as follows (UBE2T-specific sequences are underlined): forward primer: 5'-AAAGGATCCGCCACCATG CAGAGAGCTTCAC-3' and reverse primer: 5'-AAACTC GAGAACATCAGGATGAAATTTCTTTTCTATG-3'. The amplified UBE2T cDNA was then digested with BamHI/ XhoI and inserted into vector (Invitrogen) to construct pENTR201-UBE2T-FLAG vector. The Gateway Technology (Invitrogen) was then used to transfer UBE2T cDNA into the pCSII-EF-RfA (RIKEN, RDB04387), a gift from Dr. Hiroyuki Miyoshi, RIKEN (29) to generate lentiviral expression vector.

Lentivirus production and SAS cell infection. Lentivirus particles were produced by transfecting 293FT cells with the expression vectors (pCSII-EF-RfA-EMPTY, pCSII-EF-UBE2T) and packaging vectors (pCMV-VSV-G-RSV-Rev [RIKEN, RDB04393] and pCAG-HIVgp [RIKEN, RDB04394]) as previously reported (30) to produce empty lentivirus (negative control) and lentivirus expressing UBE2T. The media were refreshed 24 h post-transfection, and the supernatants containing viral particles were concentrated for 7 days at 4°C using a Lenti-X Concentrator (Takara). The concentrated viral particles were then used to infect the SAS-Fucci cells as described previously (31).

Immunoblotting analysis. Cell lysates from the SAS-Fucci cells infected with pCSII-EF-RfA-EMPTY or pCSII-EF-UBE2T lentivirus were prepared using 50 mM Tris-HCl buffer pH 7.5, 150 mM NaCl, 1% NP-40 containing Protease Inhibitor Cocktail (Nacalai Tesque). The protein concentration in obtained lysates was determined by using BCA Protein Assay Kit (Thermo Fisher Scientific). Cell lysates (47  $\mu$ g of total proteins/lane) were then separated on 10% SDS-PAGE, followed by transfer onto polyvinylidene fluoride membranes (Merck). The membranes were blocked with 5% skim milk (FUJIFILM Wako) for 30 min at room temperature and incubated with mouse monoclonal anti-FLAG M2 antibody (dilution 1:5,000, cat. no. F1804, Sigma-Aldrich) and rabbit polyclonal anti-α-tubulin (dilution 1:10,000, cat. no. ab4074, Abcam) overnight at 4°C. The membranes were then incubated with anti-mouse IgG HRP-linked antibody (goat, dilution 1:5,000, cat. no. 7074S, Cell Signaling Technology) or anti-rabbit IgG HRP-linked antibody (goat, dilution 1:5,000, cat. no. 7074S, Cell Signaling Technology) for 1 h at room temperature. Target proteins were detected with Chemiluminescence Kit (ECL detection reagent; Cytiva) and visualized with a Fusion Solo S Imaging System (Vilber).

Chamber migration assay. The SAS-Fucci cells infected with pCSII-EF-RfA-EMPTY or pCSII-EF-UBE2T lentivirus were seeded onto the upper chamber of a 24-well culture insert with 8-μm pore filter (BD Bioscience) and allowed to migrate for 48 h. The filters were then stained with DiffQuik (Sysmex), and non-migrated cells were removed with a cotton swab. Migrated cells on the bottom side of the chamber were photographed using an All-in-One microscope (BZ-710, Keyence) and counted with ImageJ software (National Institute of Health) (32).

To examine the effect of IL-6 on OSCC cell migration, SAS-Fucci cells infected with pCSII-EF-RfA-EMPTY lentivirus were seeded on 6-well plate, and incubated for 18 h followed by treatment without or with IL-6 (final concentration: 10 ng/ml) for 72 h, collected and seeded into migration chamber with 8- $\mu$ m pore filter (Corning) in 24-well plate. Cells were then allowed to migrate for 48 h. The concentration of IL-6 in medium was maintained during migration. Staining and image acquisition were done as described above.

To examine the effect of ruxolitinib on OSCC cell migration, SAS-Fucci cells infected with pCSII-EF-UBE2T lentivirus were seeded on 6-well plate, and incubated for 18 h followed by treatment without or with ruxolitinib (final concentration: 1  $\mu$ M) for 72 h. The cells were then collected, seeded into migration chamber with 8- $\mu$ m pore filter (Corning) in 24-well plate and allowed to migrate for 48 h. The concentration of ruxolitinib in the medium was maintained during migration. Staining and image acquisition were done as described above.

The brightness of representative images of migrated cells were adjusted with Adobe Photoshop 25 (Adobe) and used for figure preparation. The experiments were performed in triplicates and repeated twice.

RNA extraction and RT-qPCR analysis. Total RNA was extracted using Sepasol-RNA I Super G (Nacalai Tesque) or RNeasy Plus Mini Kit (Qiagen). The RNA was then reverse transcribed using ReverTraAce qPCR RT Master Mix (TOYOBO Life Science) according to the manufacturer's protocol. The RT-qPCR was performed with the Step One Plus Real-Time PCR System (Applied Biosystems) or QuantStudio 3 (Applied Biosystems) using gene-specific primers PowerUp SYBR Green Master Mix (Applied Biosystems). The relative-standard curve method was used to determine the relative expression of target genes (33). All expression data were normalized to the expression of  $\beta$ -actin. The genes and corresponding primer sequences are listed in Table SI. The experiments were performed in triplicates and repeated twice.

RNA sequencing and data analysis. Total RNA from SAS-Fucci cells was prepared using an RNeasy Plus Mini kit (Qiagen). The quality of RNA was evaluated using an Agilent 4200 TapeStation (Agilent). A cDNA library was prepared using TruSeq Stranded mRNA Kit (Illumina). The quality of the library was then evaluated with KAPA Library Quantification Kit (Roche) followed by sequencing NextSeq 500/550 High Output Kit v2.5 (Illumina, 75 cycles pair-end, 40/40 cycles). The average read size of 58 million. FASTQ files were processed with bcl2fastq software (Illumina Inc.) and reads were aligned against the human genome (GRCh38/hg38) using CLC Genomics Workbench version 12.0.2

(Qiagen). Normalized gene expression data, the raw TPM values were applied to GeneString version 14.9.1 (Agilent). For data analysis, TPM values were log<sub>2</sub>-transformed after adding 1, and *z*-scores were calculated.

Gene set enrichment analysis (GSEA) was performed using GSEA version 4.2.3 and previously curated gene sets (34,35). Gene Ontology (GO) analysis was performed using 'Database for Annotation, Visualization, and Integrated Discovery' (36). The raw RNA sequencing data have been deposited with links to BioProject accession number PRJDB20207 in the DNA Data Bank of Japan (DDBJ) BioProject database.

Protein interaction analysis. The protein-protein interaction network of differentially expressed genes (DEGs) was constructed using 'Search Tool for the Retrieval of Interacting Genes/Proteins' (STRING; http://string-db.org) version 12.0 (37). The interaction was considered statistically significant at an interaction score >0.4.

Statistical analysis. Significant differences between means were determined by two-tailed unpaired Student t-test using Prism software version 10.3.1 (GraphPad). Values are presented as mean ± SD. P<0.05 was considered to indicate a statistically significant difference. The significances of gene sets identified by GSEA were based on normalized enrichment scores (NES) and nominal (NOM) P-values.

#### Results

UBE2T is a poor prognostic factor associated with the development and progression of head and neck cancer. To identify factors critical for the progression of head and neck cancer, we performed an analysis using the GEPIA web server. We focused on the top 500 genes with elevated expression in head and neck cancer tissues compared with those in normal tissues and evaluated their prognostic significance using the KM-plotter database for patients with HNSCC. We identified 64 genes whose expression was significantly associated with a poor prognosis and had hazard ratios greater than 1.5 (Table SII). Further analysis of these 64 poor prognostic factors using the GEPIA Stage Plot revealed that UBE2T had the strongest correlation (F-value=5.02) with head and neck cancer stage progression (Table SIII). The results of this unbiased screening, focusing on UBE2T, are summarized in Fig. 1. UBE2T expression was significantly higher in HNSCC tumor tissues than in normal tissues (Fig. 1A). There was also a significant association between high UBE2T expression levels and poor prognosis in patients with HNSCC, as revealed by KM-plotter analysis (Fig. 1B), as well as the strongest correlation between UBE2T expression and the pathological stage of HNSCC (Fig. 1C). Therefore, we concluded that UBE2T is an unfavorable prognostic factor whose expression is elevated during the development and progression of head and neck cancer and can be considered a potential target for the treatment of HNSCC.

UBE2T enhances the motility of oral cancer cells via the induction of EMT. We next investigated the functional role of UBE2T in OSCC using the SAS-Fucci cell line. We established SAS-Fucci oral cancer cells expressing UBE2T (hereafter

termed 'UBE2T SAS cells') (Fig. 2A) and performed chamber migration assay. UBE2T SAS cells exhibited significantly enhanced motility compared with SAS-Fucci oral cancer cells infected with empty lentivirus (hereafter termed 'Control SAS cells') (Fig. 2B and C), suggesting that UBE2T promotes the motility of oral cancer cells.

To examine whether UBE2T induces EMT in OSCC cells, we performed RT-qPCR to analyze the expression of EMT marker genes in UBE2T SAS cells. Compared with Control SAS cells, UBE2T SAS cells showed decreased expression of the epithelial cell marker E-cadherin (Fig. 3A), accompanied by increased expression of the mesenchymal cell marker vimentin (Fig. 3B).

To further explore the molecular changes induced by UBE2T, we performed RNA sequencing on Control and UBE2T SAS cells, followed by GSEA (Table SIV). Increased expression of UBE2T resulted in enrichment of genes associated with the 'HALLMARK\_EMT' (Fig. 3C; Table SIV), indicating that UBE2T induces EMT in OSCC cells. Collectively, these findings suggest that UBE2T induces EMT, which contributes to the enhanced motility of OSCC cells.

UBE2T upregulates the expression of various factors associated with motility and EMT in oral cancer cells. To determine the factors and biological processes regulated by UBE2T in oral cancer cells, we focused on DEGs whose expression was upregulated more than threefold in UBE2T SAS cells compared with Control SAS cells and identified 62 DEGs upregulated in UBE2T SAS cells (Table SV). Further GO analysis of these 62 DEGs revealed the enrichment in 'positive regulation of cell motility' and 'intermediate filament organization' terms which were among the top-ranked categories (Fig. 4A). We have also examined the expression of already reported, several motility- and EMT-related factors, including ankyrin repeat domain 1 (ANKRD1) (38), endothelin-1 (39), matrix metalloproteinase-9 (MMP-9) (40), and plasminogen activator, urokinase (PLAU) (41). RT-qPCR analysis revealed increased expression levels of ANKRD1 (Fig. 4B), endothelin-1 (Fig. 4C), MMP-9 (Fig. 4D), and PLAU (Fig. 4E) in UBE2T SAS cells compared with Control SAS cells. These results suggest that UBE2T promotes the expression of various factors associated with motility and EMT in OSCC cells.

UBE2T upregulates the IL-6 signaling pathway in oral cancer cells. To identify the key factors mediating UBE2T-induced motility and EMT, we performed STRING analysis on the 62 DEGs whose expression was upregulated by more than threefold in UBE2T SAS cells compared with Control SAS cells. Among the 62 DEGs upregulated in UBE2T SAS cells, IL-6 was identified as the central hub (Fig. 5A). Additionally, the protein-protein network revealed the interaction of IL-6 with mesenchymal cell marker genes, such as vimentin, endothelin-1, MMP-9, and PLAU (Fig. 5A), whose expression was upregulated in UBE2T SAS cells (Figs. 3B and 4C-E).

IL-6/JAK/signal transducer and activator of transcription 3 (STAT3) signaling is known for its role in cancer progression, including OSCC (42,43). GSEA revealed the possibility of IL-6/JAK/STAT3 signaling pathway activation in UBE2T SAS cells, ranking sixth among the enriched gene



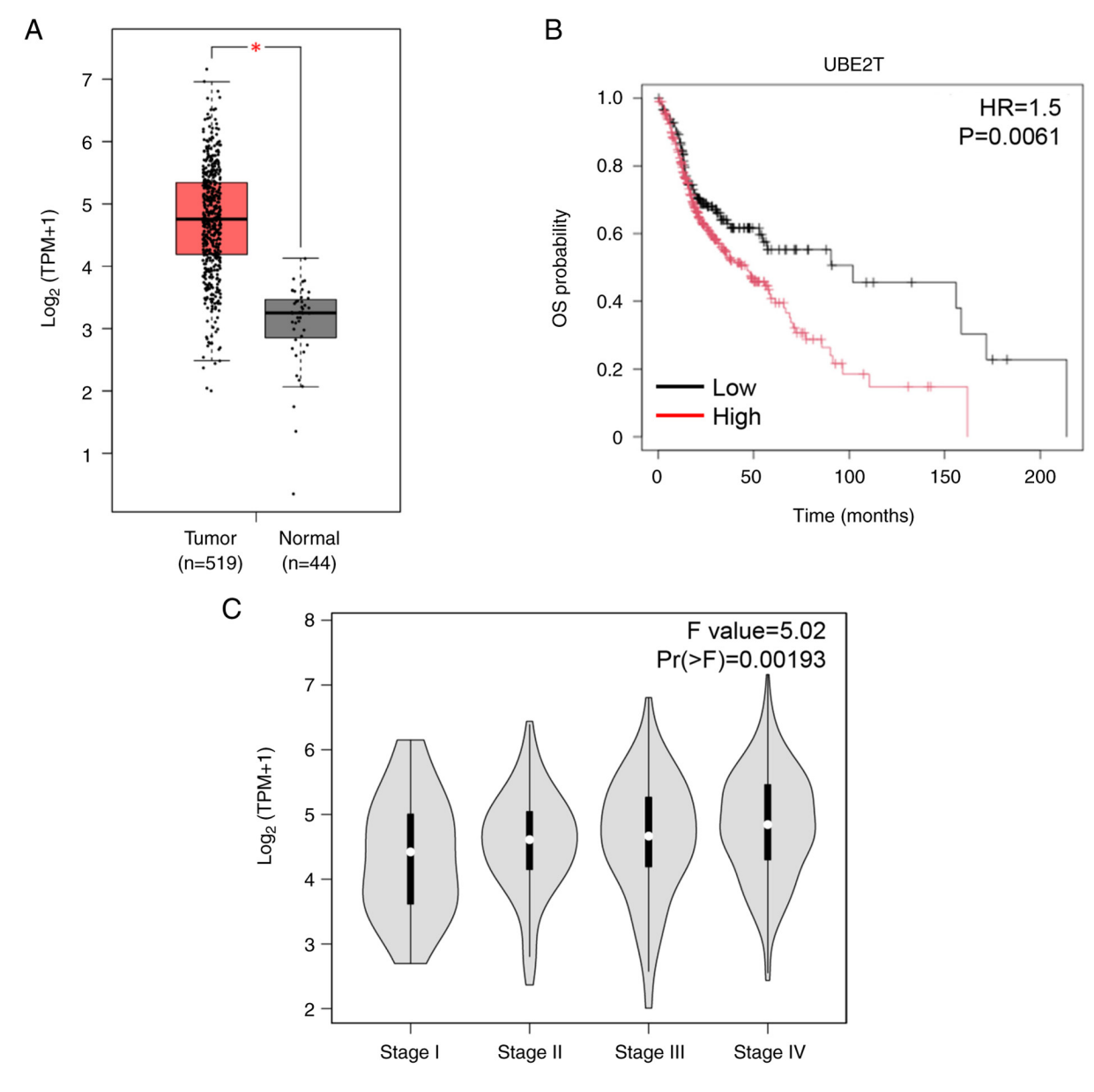


Figure 1. UBE2T correlates with poor prognosis and progression of HNSCC. (A) Analysis of UBE2T expression in HNSCC tumor (Tumor; red) and normal tissues (Normal; gray) using GEPIA web server. Values represent first log<sub>2</sub>(TPM+1) transformed expression data. HNSCC tumor tissues (n=519), normal tissues (n=44). Statistical analysis: one-way ANOVA; \*P<0.05. (B) Correlation between UBE2T expression and OS of patients with HNSCC. Kaplan-Meier survival plot of two patient cohorts with low (black) and high (red) UBE2T expressions. HR and P-values are shown. (C) Violin plots showing correlation between UBE2T expression and pathological stages (stage I to IV) of HNSCC analyzed using GEPIA web server. Values represent first log<sub>2</sub>(TPM+1) transformed expression data. Statistical analysis: one-way ANOVA; F and P values are shown. GEPIA, Gene Expression Profiling Interactive Analysis; HNSCC, head and neck squamous cell carcinoma; HR, hazard ratio; OS, overall survival; TPM, transcripts per million; UBE2T, ubiquitin-conjugating enzyme E2 T.

sets (Fig. 5B; Table SIV). Furthermore, GO analysis showed enrichment in terms related to 'positive regulation of tyrosine phosphorylation of STAT protein' (Fig. 4A), supporting GSEA results. Additionally, RT-qPCR revealed that IL-6 expression was upregulated in UBE2T SAS cells (Fig. 5C), suggesting that UBE2T regulates the IL-6/JAK/STAT3 signaling pathway in OSCC cells.

IL-6 induces EMT and promotes migration in oral cancer cells. To examine the role of IL-6 in the induction of EMT, Control SAS cells were cultured in the absence or presence of recombinant IL-6, and EMT-related gene expression levels were analyzed. RT-qPCR revealed that IL-6 treatment decreased the expression of the epithelial cell marker

E-cadherin (Fig. 6A) and increased the expression of the mesenchymal cell marker vimentin (Fig. 6B), suggesting that IL-6 induces EMT in oral cancer cells. We also examined the migration of oral cancer cells after treatment with IL-6. The chamber migration assay demonstrated that IL-6 enhanced the motility of Control SAS cells (Fig. 6C and D), revealing that IL-6 not only induced EMT but also promoted motility in OSCC cells. Collectively, these results indicate that IL-6, which is upregulated by increased levels of UBE2T, is critical for maintaining mesenchymal traits and motility in OSCC cells.

Inhibition of JAK induces mesenchymal-epithelial transition and suppresses migration in oral cancer cells. As our RNA

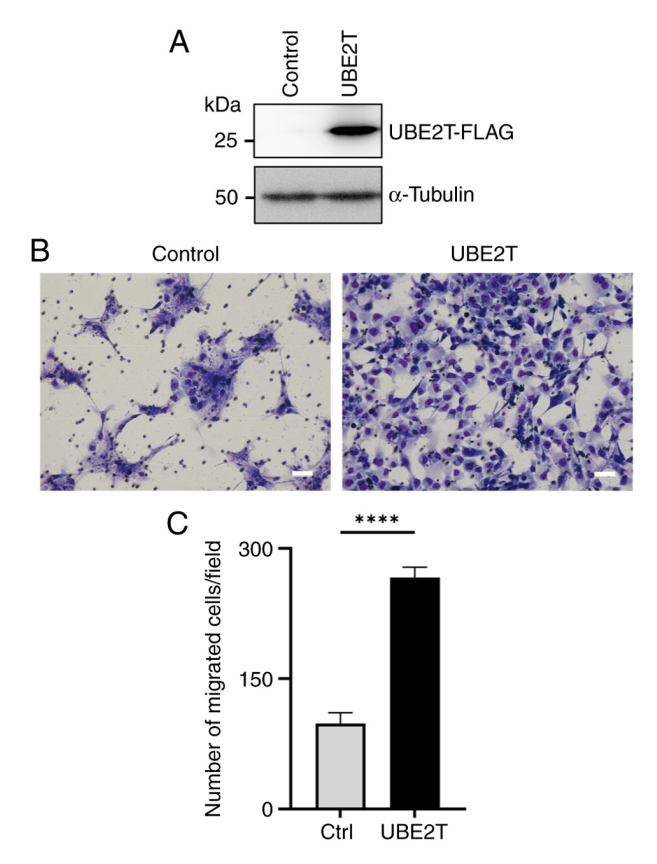


Figure 2. UBE2T enhances migration of oral cancer cells. Ctrl SAS cells and UBE2T SAS cells (UBE2T) were established by infecting SAS-Fucci cells with empty lentivirus or lentivirus expressing FLAG-tagged UBE2T followed by chamber migration assay. (A) Expression of FLAG-tagged UBE2T was visualized by immunoblotting analysis using anti-FLAG M2 antibody.  $\alpha$ -tubulin was used as a loading control for cell lysate. (B and C) Migration assay of Control and UBE2T SAS cells. (B) Representative images of migrated cells are shown. Scale bars: 50  $\mu$ m. (C) Quantitative analysis of migrated cells. Data are represented as mean  $\pm$  SD. Statistical analysis: two-tailed unpaired Student's t-test; \*\*\*\*P<0.0001. Ctrl, control; UBE2T, ubiquitin-conjugating enzyme E2 T.

sequencing data suggested that IL-6/JAK/STAT3 signaling was activated by elevated UBE2T expression (Fig. 5C), we examined whether inhibition of the JAK/STAT3 pathway affected UBE2T-induced EMT. UBE2T SAS cells were treated with ruxolitinib, a selective JAK inhibitor followed by RT-qPCR analysis of EMT marker gene expression. Treatment of UBE2T SAS cells with ruxolitinib induced increased expression of an epithelial cell marker E-cadherin (Fig. 7A). Additionally, ruxolitinib decreased expression of the mesenchymal cell marker vimentin (Fig. 7B), suggesting that cells underwent mesenchymal-epithelial transition (MET), a process reversal to EMT. Moreover, ruxolitinib treatment inhibited the migration of UBE2T SAS cells compared with that of the untreated control (Fig. 7C and D). Taken together, our data suggest that UBE2T induces EMT and enhances cell motility in OSCC, potentially through regulation of the IL-6/ JAK/STAT3 signaling pathway (Fig. S1).

# Discussion

In the present study, we identified UBE2T as a poor prognostic factor for head and neck cancer, showing the strongest

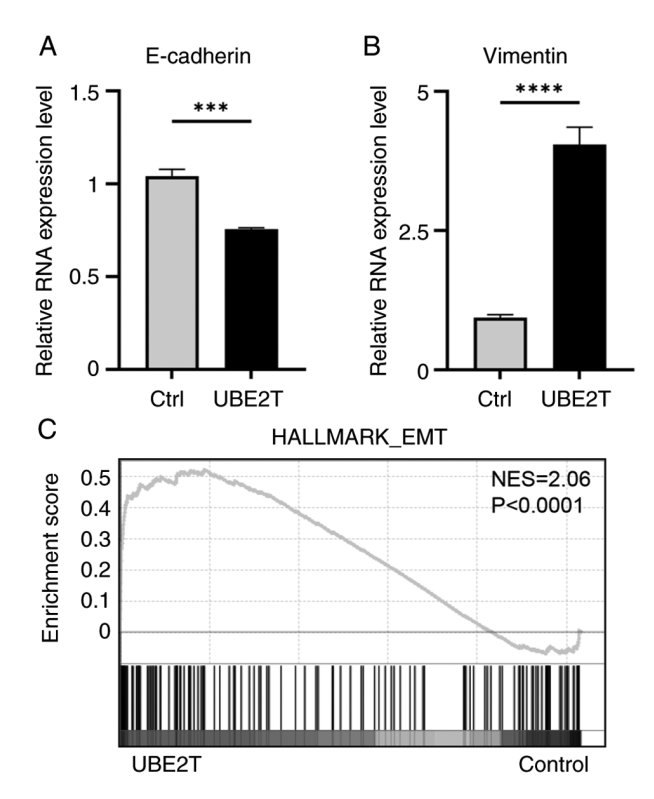


Figure 3. UBE2T induces EMT in oral cancer cells. (A and B) The expression levels of an epithelial cell marker E-cadherin and a mesenchymal cell marker vimentin in Ctrl SAS cells and UBE2T SAS cells (UBE2T) were examined using reverse transcription-quantitative PCR. Relative expression of (A) an epithelial cell marker, E-cadherin and (B) a mesenchymal cell marker, vimentin. All data are normalized to the expression of  $\beta$ -actin. Data are represented as mean  $\pm$  SD. Statistical analyses: two-tailed unpaired Student's t-test; \*\*\*P<0.001; \*\*\*\*P<0.0001. (C) GSEA of EMT gene signatures, comparing RNA sequencing data from Ctrl SAS cells with UBE2T SAS cells (UBE2T). n=2 per group. Ctrl, control; EMT, epithelial-mesenchymal transition; GSEA, gene set enrichment analysis; NES, normalized enrichment score; P-val, nominal P-value from GSEA; UBE2T, ubiquitin-conjugating enzyme E2 T.

correlation with cancer stage progression through bioinformatics analysis. Previous studies have shown that UBE2T overexpression promotes tumor growth, enhances cell proliferation, migration, and invasion, and regulates cancer stem cell properties across multiple cancer types (19). Our data also revealed that increased UBE2T expression enhanced the motility and induced EMT in OSCC cells, which is in agreement with previous findings, identifying UBE2T as a poor prognostic factor associated with cancer development and progression, particularly in head and neck cancers (44).

RNA sequencing and subsequent analyses showed that UBE2T upregulated various factors associated with motility and EMT in OSCC cells. We identified several genes that were upregulated in UBE2T SAS cells, such as ANKRD1, endothelin-1, MMP-9, and PLAU, which have been implicated in the induction of EMT and cancer metastasis (38-41). Upregulated ANKRD1 expression has been linked to TGF-β signaling and cytoskeletal rearrangements associated with EMT (38). Additionally, endothelin-1 has been shown to induce EMT through the extracellular signal-regulated kinase and PI3K pathways (39). MMP-9 promotes the degradation of the extracellular matrix, facilitating cancer cell invasion (45), whereas PLAU activates the proteolytic cascades involved



Α

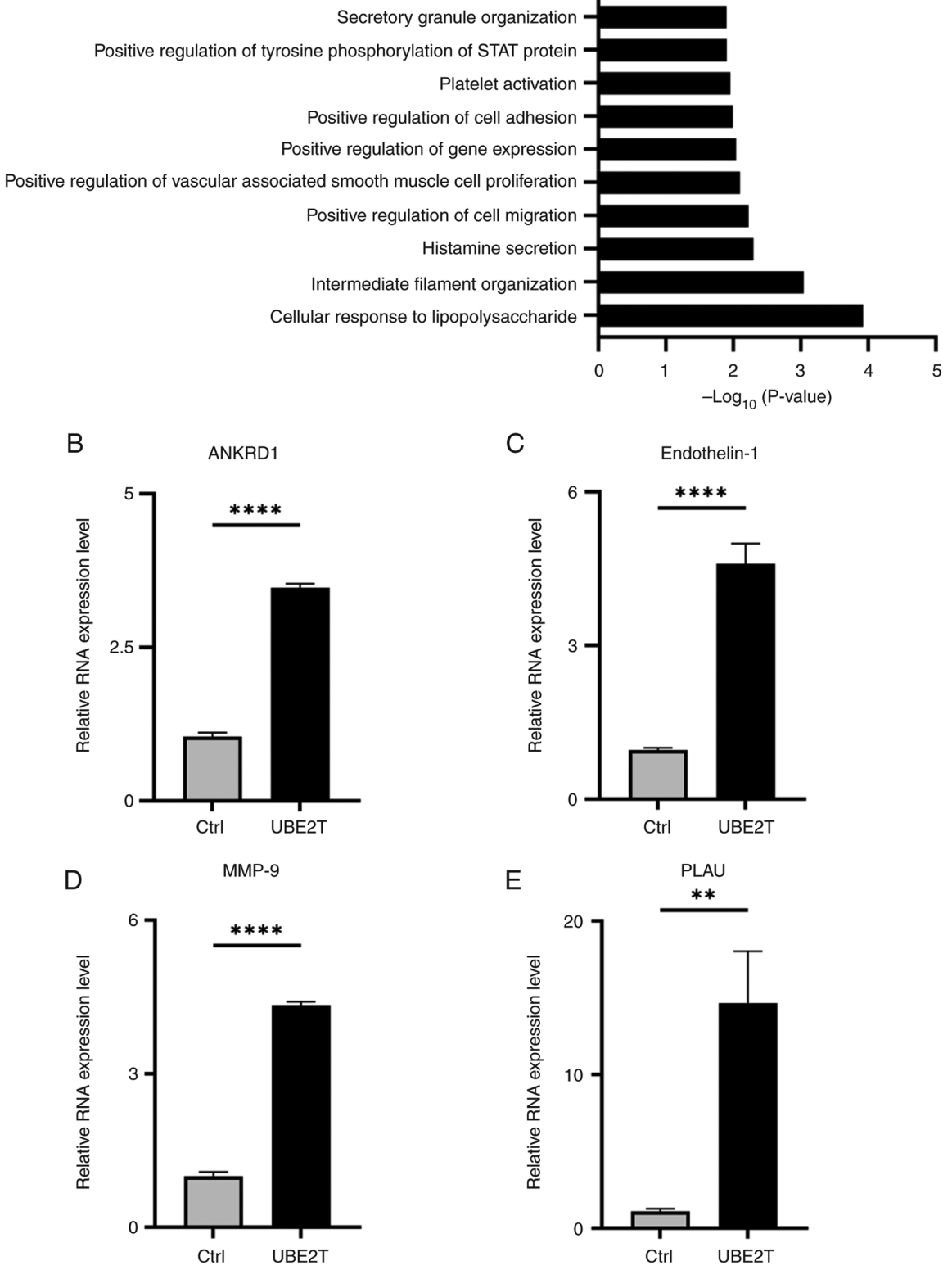


Figure 4. UBE2T upregulates the expression of mesenchymal cell markers associated with motility and epithelial-mesenchymal transition. (A) Gene Ontology functional enrichment analysis of 62 differentially expressed genes upregulated in UBE2T SAS cells compared with Ctrl SAS cells. (B-E) Expression of various mesenchymal cell markers in Ctrl SAS cells and UBE2T SAS cells (UBE2T) were examined by reverse transcription-quantitative PCR. Relative expression of (B) ANKRD1, (C) endothelin-1, (D) MMP-9 and (E) PLAU. All data are normalized to the expression of  $\beta$ -actin. Data are represented as mean  $\pm$  SD. Statistical analyses: two-tailed unpaired Student's t-test; \*\*P<0.001; \*\*\*\*P<0.0001. ANKRD1, ankyrin repeat domain 1; Ctrl, control; MMP-9, matrix metalloproteinase-9; PLAU, plasminogen activator, urokinase; UBE2T, ubiquitin-conjugating enzyme E2 T.

in tissue remodeling (41). The expression of the identified genes was upregulated in UBE2T SAS cells, suggesting that, in OSCC cells, UBE2T induces EMT via upregulation of

multiple motility- and EMT-associated genes. Further experiments are required to validate their functional contribution to OSCC progression.

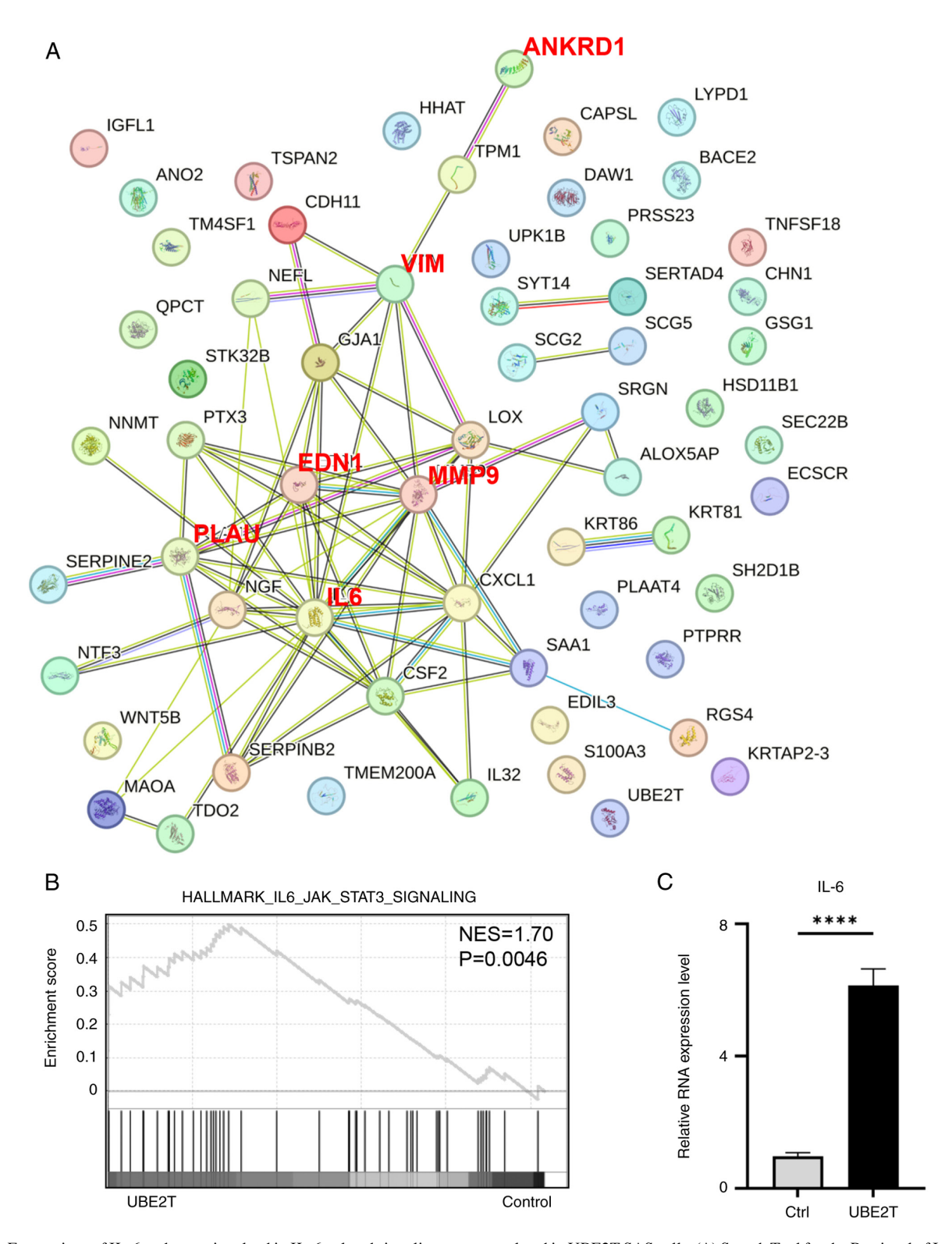


Figure 5. Expressions of IL-6 and genes involved in IL-6-related signaling are upregulated in UBE2T SAS cells. (A) Search Tool for the Retrieval of Interacting Genes analysis of 62 differentially expressed genes upregulated in UBE2T SAS cells. Red font indicates previously reported factors, associated with cancer cell migration and epithelial-mesenchymal transition. (B) GSEA of 'HALLMARK\_IL6\_JAK\_STAT3\_SIGNALING' gene set comparing RNA sequencing data from Ctrl SAS cells and UBE2T SAS cells (UBE2T). n=2 per group. (C) Relative expression of IL-6 in Control SAS cells (Ctrl) and UBE2T SAS cells (UBE2T). Data are normalized to the expression of  $\beta$ -actin. Data are represented as mean  $\pm$  SD. Statistical analysis: two-tailed unpaired Student's t-test; \*\*\*\*\*P<0.0001. ANKRD1, ankyrin repeat domain 1; Ctrl, control; EDN1, endothelin-1; GSEA, gene set enrichment analysis; IL-6/IL6, interleukin-6; JAK, Janus protein tyrosine kinase; MMP9, matrix metalloproteinase-9; NES, normalized enrichment score; PLAU, plasminogen activator, urokinase; P, nominal P-value from GSEA; STAT3, signal transducer and activator of transcription 3; UBE2T, ubiquitin-conjugating enzyme E2 T; VIM, vimentin.

Our RNA sequencing data suggested that the IL-6/JAK/ STAT3 signaling pathway was upregulated in UBE2T SAS cells. The IL-6/JAK/STAT3 pathway has been implicated in cancer progression and induction of EMT in various



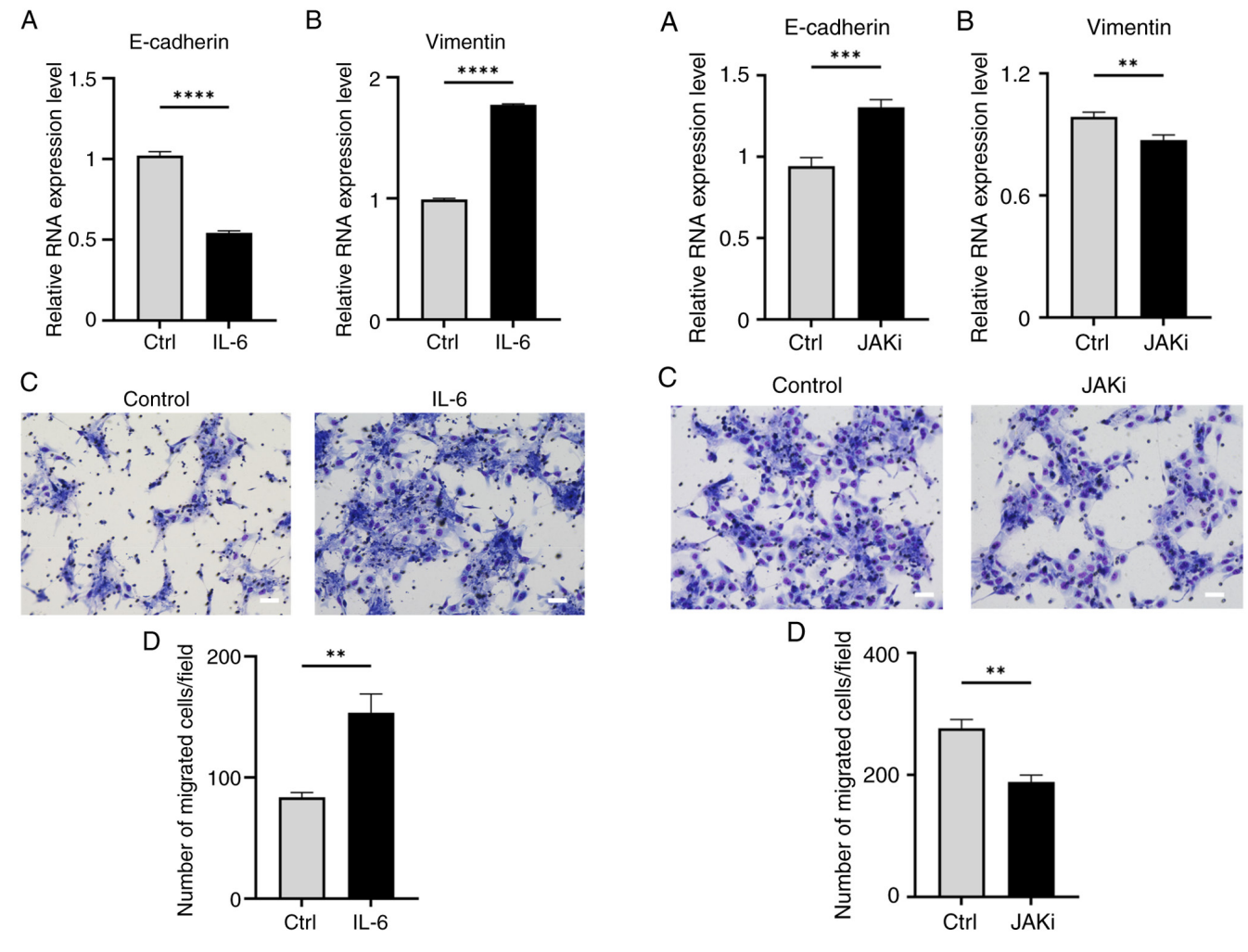


Figure 6. IL-6 induces epithelial-mesenchymal transition and enhances migration of oral cancer cells. SAS cells were cultured in the absence (Ctrl) or presence of IL-6 (IL-6) for 72 h followed by (A and B) reverse transcription-quantitative PCR and (C and D) chamber migration assay. Relative expression levels of (A) an epithelial cell marker, E-cadherin and (B) a mesenchymal cell marker, vimentin. All data are normalized to the expression of  $\beta$ -actin. (C) Representative images of migrated cells treated without (Ctrl) or with IL-6 (IL-6) are shown. Scale bars: 50  $\mu$ m. (D) Quantitative analysis of migrated cells. All data are represented as mean  $\pm$  SD. Statistical analyses: two-tailed unpaired Student's t-test; \*\*P<0.01, \*\*\*\*\*P<0.0001. Ctrl, control; IL-6, interleukin-6.

Figure 7. JAKi induces mesenchymal-epithelial transition and suppresses migration of oral cancer cells. UBE2T SAS cells were cultured in the absence (Ctrl) or presence of ruxolitinib, a JAKi for 72 h followed by (A and B) reverse transcription-quantitative PCR and (C and D) chamber migration assay. Relative expression levels of (A) an epithelial cell marker, E-cadherin and (B) a mesenchymal cell marker, vimentin. All data are normalized to the expression of  $\beta$ -actin. (C) Representative images of migrated cells treated without (Ctrl) or with JAKi are shown. Scale bars: 50  $\mu$ m. (D) Quantitative analysis of migrated cells. All data are represented as mean  $\pm$  SD. Statistical analyses: two-tailed unpaired Student's t-test; \*\*P<0.01, \*\*\*P<0.001. Ctrl, control; JAKi, Janus protein tyrosine kinase inhibitor.

malignancies, including OSCC (42). RNA sequencing data suggested that the IL-6/JAK/STAT3 signaling pathway mediates UBE2T-induced cell motility and EMT. Our findings suggest that UBE2T regulates this pathway, leading to enhanced motility and mesenchymal traits in OSCC cells.

The present results indicate an important role for IL-6 in the induction of mesenchymal phenotypes and motility of oral cancer cells, as treatment with IL-6 induced EMT and promoted cancer cell migration. These findings were in agreement with the previous reports highlighting the importance of IL-6 in promoting EMT and cancer progression by affecting cancer cell invasion and drug resistance (43). IL-6 has been shown to activate the JAK/STAT3 signaling pathway, which is known to induce EMT in various cancer types, including OSCC (42). Indeed, the inhibition of JAK with the selective JAK inhibitor ruxolitinib induced MET and suppressed the migration of UBE2T SAS cells, confirming the involvement

of the JAK/STAT3 signaling pathway. Thus, targeting IL-6 with neutralizing antibodies or selective JAK inhibitors could potentially address the challenges associated with metastasis and drug resistance in OSCC treatment (43). Indeed, previous reports have shown that targeting IL-6 or its downstream effectors can inhibit tumor growth and metastasis in various cancer models (42,46). Additionally, combining therapies targeting IL-6 with conventional treatments may enhance therapeutic efficacy in patients with OSCC.

Inhibition of UBE2T activity could potentially reverse oncogenic effects, such as EMT and cancer cell motility, suppressing tumor growth, metastasis, and drug resistance. Recent studies have demonstrated that UBE2T inhibition can suppress tumorigenesis and tumor growth in HNSCC by inhibiting nuclear factor- $\alpha$ B signaling and inducing ferroptosis (47). Furthermore, UBE2T inhibition has shown promise in other cancer types such as gastric cancer (48) and glioblastoma (14),

where it suppresses Wnt-mediated signaling and tumor progression. Given the multifaceted roles of UBE2T in tumorigenesis, the development of its specific inhibitors could provide a novel therapeutic approach, either as standalone treatments or in combination with existing therapies, to improve outcomes in cancer patients.

Our study has several limitations that require further investigation. First, although our findings suggest potential roles for ANKRD1, endothelin-1, MMP-9, and PLAU in UBE2T-driven EMT, future studies involving targeted knockdown or pathway inhibition are needed to clarify their functional relevance and interactions with canonical EMT signaling pathways. Second, the precise mechanism by which UBE2T upregulates IL-6 expression remains unclear. Recent findings by Pu et al have suggested that UBE2T mediates the ubiquitination of sorbin and SH3 domain-containing 3, thereby enhancing IL-6/STAT3 signaling and promoting the progression of lung adenocarcinoma (49). This mechanism may provide insights into how UBE2T activates IL-6 signaling; however, further studies are needed to identify the targets of UBE2T-mediated ubiquitination in the context of OSCC. Third, in vivo studies are required to confirm the relevance of our findings in a pathophysiological context. Additionally, the potential crosstalk between the UBE2T/IL-6 axis and other signaling pathways involved in OSCC progression should be explored.

In conclusion, our study identified UBE2T as a factor that promotes EMT and motility in OSCC cells through the upregulation of IL-6 expression. These findings contribute to our understanding of OSCC progression and may lead to the development of new therapeutic strategies that target the UBE2T/IL-6 axis.

# Acknowledgements

The authors would like to thank Dr Hiroyuki Miyoshi (RIKEN, deceased) for the lentiviral vectors, Dr Miki Yokoyama and Dr Haruka Ibi (Institute of Science Tokyo) for technical assistance and Dr Miho Kobayashi (Institute of Science Tokyo) for critical discussion.

## **Funding**

This study was conducted by a research program of the Japan Agency for Medical Research and Development (grant nos. 22ama221205 and 24ama221238h0001 to TW). This work was also supported in part by JSPS KAKENHI (grant nos. JP23H03070 and JP23H05486 to TW, JP23K0913 to KAPI and JP23K15962 to KT), and by MEXT, the Establishment of University Fellowships Towards the Creation of Science Technology Innovation (grant no. JPMJFS2109 to JL) and JST SPRING (grant no. JPMJFS2120 to JL).

### Availability of data and materials

The RNA sequencing data generated in the present study may be found in the BioProject database under accession number PRJDB20207 or at the following URL: https://www.ncbi.nlm.nih.gov/bioproject/?term=PRJDB20207. The other data generated in the present study may be requested from the corresponding author.

#### **Authors' contributions**

AW, JL, KT, KAPI and TW conceived and designed the experiments. AW, JL, KI and SI performed the experiments. AW, JL, SI, KO, SH, TA, KAPI and TW analyzed and interpreted the data. AW, JL, KI and SI performed the data acquisition. AW, JL, KAPI and TW wrote the manuscript. AW, JL, KI, SI, KO, SH, TA, KT, KAPI and TW conducted the manuscript revision/review. AW, JL, SI, KT, KAPI and TW confirm the authenticity of all the raw data. All authors read and approved the final version of the manuscript.

## Ethics approval and consent to participate

The molecular biology experimental procedures were approved by the Genetically Modified Organisms Safety Committee of Institute of Science Tokyo (approval nos. G2019-026C9 and G 2024-007C5).

## **Patients consent for publication**

Not applicable.

# **Competing interests**

The authors declare that they have no competing interests.

#### References

- 1. Biray Avci C, Goker Bagca B, Nikanfar M, Takanlou LS, Takanlou MS and Nourazarian A: Tumor microenvironment and cancer metastasis: Molecular mechanisms and therapeutic implications. Front Pharmacol 15: 1442888, 2024.
- Li Y, Liu F, Cai Q, Deng L, Ouyang Q, Zhang XH and Zheng J: Invasion and metastasis in cancer: Molecular insights and therapeutic targets. Sig Transduct Target Ther 10: 57, 2025.
- Miyazono K, Katsuno Y, Koinuma D, Ehata S and Morikawa M: Intracellular and extracellular TGF-β signaling in cancer: Some recent topics. Front Med 12: 387-411, 2018.
- Xie Y, Wang X, Wang W, Pu N and Liu L: Epithelial-mesenchymal transition orchestrates tumor microenvironment: Current perceptions and challenges. J Transl Med 23: 386, 2025.
- Robinson DR, Wu YM, Lonigro RJ, Vats P, Cobain E, Everett J, Cao X, Rabban E, Kumar-Sinha C, Raymond V, et al: Integrative clinical genomics of metastatic cancer. Nature 548: 297-303, 2017.
- Bray F, Laversanne M, Sung H, Ferlay J, Siegel RL, Soerjomataram I and Jemal A: Global cancer statistics 2022: GLOBOCAN estimates of incidence and mortality worldwide for 36 cancers in 185 countries. CA Cancer J Clin 74: 229-263, 2024.
- 7. Hernández-Morales A, González-López BS, Scougall-Vilchis RJ, Bermeo-Escalona JR, Velázquez-Enríquez U, Islas-Zarazúa R, Márquez-Rodríguez S, Sosa-Velasco TA, Medina-Solís CE and Maupomé G: Lip and oral cavity cancer incidence and mortality rates associated with smoking and chewing tobacco use and the human development index in 172 countries worldwide: An ecological study 2019-2020. Healthcare (Basel) 11: 1063, 2023.
- 8. Kinoshita N, Tomioka H, Oikawa Y, Fukawa Y, Ikeda T and Harada H: A case of sclerosing odontogenic carcinoma of the mandible with a review of the literature. J Oral Sci 65: 281-283, 2023.
- Tranby EP, Heaton LJ, Tomar SL, Kelly AL, Fager GL, Backley M and Frantsve-Hawley J: Oral cancer prevalence, mortality, and costs in Medicaid and commercial insurance claims data. Cancer Epidemiol Biomarkers Prev 31: 1849-1857, 2022.
- Miranda-Filho A and Bray F: Global patterns and trends in cancers of the lip, tongue and mouth. Oral Oncol 102: 104551, 2020.



- 11. Tan Y, Wang Z, Xu M, Li B, Huang Z, Qin S, Nice EC, Tang J and Huang C: Oral squamous cell carcinomas: State of the field and emerging directions. Int J Oral Sci 15: 44, 2023
- 12. Katsuno Y and Derynck R: Epithelial plasticity, epithelial-mesenchymal transition, and the TGF-β family. Dev Cell 56: 726-746,
- 13. Ling H, Xiao S, Lei Y, Zhou Y, Tan J, Chen X, Ma D, Liang C, Liu Q, Liu W and Zeng T: The advancement of ubiquitination regulation in apoptosis, ferroptosis, autophagy, drug resistance and treatment of cancer. Arch Biochem Biophys 771: 110497, 2025.
- 14. Wang Y, Gao G, Wei X, Zhang Y and Yu J: UBE2T promotes temozolomide resistance of glioblastoma through regulating the Wnt/β-catenin signaling pathway. Drug Des Devel Ther 17: 1357-1369, 2023.
- Peng J, Dai X, Zhang T, Hu G, Cao H, Guo X, Fan H, Chen J, Tang W and Yang F: Copper as the driver of the lncRNA-TCONS-6251/miR-novel-100/TC2N axis: Unraveling ferroptosis in duck kidney. Int J Biol Macromol 282 (Pt 2):
- 136797, 2024. 16. Chen J, Dai X, Xing C, Zhang Y, Cao H, Hu G, Guo X, Gao X, Liu P and Yang F: Cooperative application of transcriptomics and ceRNA hypothesis: lncRNA-00742/ miR-116 targets CD74 to mediate vanadium-induced mitochondrial apoptosis in duck liver. J Hazard Mater 480: 135904, 2024.
- 17. Liu F, Chen J, Li K, Li H, Zhu Y, Zhai Y, Lu B, Fan Y, Liu Z, Chen X, et al: Ubiquitination and deubiquitination in cancer: From mechanisms to novel therapeutic approaches. Mol Cancer 23: 148, 2024.
- 18. Dutta R, Guruvaiah P, Reddi KK, Bugide S, Reddy Bandi DS, Edwards YJK, Singh K and Gupta R: UBE2T promotes breast cancer tumor growth by suppressing DNA replication stress.

  NAR Cancer 4: zcac035, 2022.

  19. Ma N, Li Z, Yan J, Liu X, He L, Xie R and Lu X: Diverse roles of
- UBE2T in cancer (Review). Oncol Rep 49: 69, 2023.
- 20. Yin H, Wang X, Zhang X, Zeng Y, Xu Q, Wang W, Zhou F and Zhou Y: UBE2T promotes radiation resistance in non-small cell lung cancer via inducing epithelial-mesenchymal transition and the ubiquitination-mediated FOXO1 degradation. Cancer Lett 494: 121-131, 2020.
- 21. Ho NPY, Leung CON, Wong TL, Lau EYT, Lei MML, Mok EHK, Leung HW, Tong M, Ng IOL, Yun JP, et al: The interplay of UBE2T and Mule in regulating Wnt/β-catenin activation to promote hepatocellular carcinoma progression. Cell Death Dis 12: 148, 2021
- 22. Hao P, Kang B, Li Y, Hao W and Ma F: UBE2T promotes proliferation and regulates PI3K/Akt signaling in renal cell carcinoma. Mol Med Rep 20: 1212-1220, 2019.
- 23. Kim JW, Gautam J, Kim JE, Kim JA and Kang KW: Inhibition of tumor growth and angiogenesis of tamoxifen-resistant breast cancer cells by ruxolitinib, a selective JAK2 inhibitor. Oncol Lett 17: 3981-3989, 2019.
- 24. Bai Y, Wang W, Yin P, Gao J, Na L, Sun Y, Wang Z, Zhang Z and Zhao C: Ruxolitinib alleviates renal interstitial fibrosis in UUO Mice. Int J Biol Sci 16: 194-203, 2020.
- 25. Onozato Y, Kaida A, Harada H and Miura M: Radiosensitivity of quiescent and proliferating cells grown as multicellular tumor spheroids. Cancer Sci 108: 704-712, 2017.
- 26. Sakaue-Sawano A, Kurokawa H, Morimura T, Hanyu A, Hama H, Osawa H, Kashiwagi S, Fukami K, Miyata T, Miyoshi H, et al: Visualizing spatiotemporal dynamics of multicellular cell-cycle progression. Cell 132: 487-498, 2008.
- 27. Tang Z, Li C, Kang B, Gao G, Li C and Zhang Z: GEPIA: A web server for cancer and normal gene expression profiling and interactive analyses. Nucleic Acids Res 45 (W1): W98-W102,
- 28. Győrffy B: Integrated analysis of public datasets for the discovery and validation of survival-associated genes in solid tumors. Innovation (Camb) 5: 100625, 2024.
- 29. Miyoshi H, Blömer U, Takahashi M, Gage FH and Verma IM: Development of a self-inactivating lentivirus vector. J Virol 72: 8150-8157, 1998.
- 30. Kodama S, Podyma-Inoue KA, Uchihashi T, Kurioka K, Takahashi H, Sugauchi A, Takahashi K, Inubushi T, Kogo M, Tanaka S and Watabe T: Progression of melanoma is suppressed by targeting all transforming growth factor-β isoforms with an Fc chimeric receptor. Oncol Rep 46: 197,

- 31. Takahashi K, Akatsu Y, Podyma-Inoue KA, Matsumoto T, Takahashi H, Yoshimatsu Ý, Koinuma D, Shirouzu M, Miyazono K and Watabe T: Targeting all transforming growth factor-β isoforms with an Fc chimeric receptor impairs tumor growth and angiogenesis of oral squamous cell cancer. J Biol Chem 295: 12559-12572, 2020.
- 32. Schneider CA, Rasband WS and Eliceiri KW: NIH Image to ImageJ: 25 years of image analysis. Nat Methods 9: 671-675, 2012
- 33. Pfaffl MW: Relative quantification. In: Real-time PCR. Dorak MT (ed). 1st edition. Taylor & Francis, London, 2006.
- 34. Mootha VK, Lindgren CM, Eriksson KF, Subramanian A, Sihag S, Lehar J, Puigserver P, Carlsson E, Ridderstråle M, Laurila E, et al: PGC-1alpha-responsive genes involved in oxidative phosphorylation are coordinately downregulated in human diabetes. Nat Genet 34: 267-273, 2003
- 35. Subramanian A, Tamayo P, Mootha VK, Mukherjee S, Ebert BL, Gillette MA, Paulovich A, Pomeroy SL, Golub TR, Lander ES and Mesirov JP: Gene set enrichment analysis: a knowledge-based approach for interpreting genome-wide expression profiles. Proc Natl Acad Sci USA 102: 15545-15550, 2005.
- 36. Dennis G Jr, Sherman BT, Hosack DA, Yang J, Gao W, Lane HC and Lempicki RA: DAVID: Database for annotation, visualization, and integrated discovery. Genome Biol 4: P3, 2003. 37. Szklarczyk D, Franceschini A, Wyder S, Forslund K, Heller D,
- Huerta-Cepas J, Simonovic M, Roth A, Santos A, Tsafou KP, et al: STRING v10: Protein-protein interaction networks, integrated over the tree of life. Nucleic Acids Res 43 (Database issue): D447-D452, 2015.
- 38. Xu X, Zhong D, Wang X, Luo F, Zheng X, Feng T, Chen R, Cheng Y, Wang Y and Ma G: Pan-cancer integrated analysis of ANKRD1 expression, prognostic value, and potential implications in cancer. Sci Rep 14: 5268, 2024.
- 39. Harrison M, Zinovkin D and Pranjol MZI: Endothelin-1 and its role in cancer and potential therapeutic opportunities. Biomedicines 12: 511, 2024.
- 40. Ibi H, Takahashi K, Harada H, Watabe T and Podyma-Inoue KA: Transforming growth factor-β signals promote progression of squamous cell carcinoma by inducing epithelial-mesenchymal transition and angiogenesis. Biochem Biophys Res Commun 714: 149965, 2024.
- 41. Sarno F, Goubert D, Logie E, Rutten MGS, Koncz M, Deben C, Niemarkt AE, Altucci L, Verschure PJ, Kiss A, et al: Functional validation of the putative oncogenic activity of PLAU. Biomedicines 11: 102, 2022.
- 42. Yadav A, Kumar B, Datta J, Teknos TN and Kumar P: IL-6 promotes head and neck tumor metastasis by inducing epithelial-mesenchymal transition via the JAK-STAT3-SNAIL
- signaling pathway. Mol Cancer Res 9: 1658-1667, 2011. 43. Thuya WL, Cao Y, Ho PC, Wong AL, Wang L, Zhou J, Nicot C and Goh BC: Insights into IL-6/JAK/STAT3 signaling in the tumor microenvironment: Implications for cancer therapy. Cytokine Growth Factor Rev: Jan 17, 2025 (Epub ahead of print).
- 44. Gao C, Liu YJ, Yu J, Wang R, Shi JJ, Chen RY, Yang GJ, Chen J. Unraveling the role of ubiquitin-conjugating enzyme UBE2T in tumorigenesis: A comprehensive review. Cells.4:15, 2024.
- 45. Augoff K, Hryniewicz-Jankowska A, Tabola R and Stach K: MMP9: A tough target for targeted therapy for cancer. Cancers (Basel) 14: 1847, 2022.
- 46. Kumari N, Dwarakanath BS, Das A and Bhatt AN: Role of interleukin-6 in cancer progression and therapeutic resistance. Tumour Biol 37: 11553-11572, 2016.
- 47. Cai F, Xu H, Song S, Wang G, Zhang Y, Qian J and Xu L: Knockdown of ubiquitin-conjugating enzyme E2 T abolishes the progression of head and neck squamous cell carcinoma by inhibiting NF-xb signaling and inducing ferroptosis. Curr Protein Pept Sci 25: 577-585, 2024.
- 48. Yu Z, Jiang X, Qin L, Deng H, Wang J, Ren W, Li H, Zhao L, Liu H, Yan H, et al: A novel UBE2T inhibitor suppresses Wnt/β-catenin signaling hyperactivation and gastric cancer progression by blocking RACK1 ubiquitination. Oncogene 40: 1027-1042, 2021
- 49. Pu J, Wang B, Zhang D, Wang K, Yang Z, Zhu P and Song Q: UBE2T mediates SORBS3 ubiquitination to enhance IL-6/ STAT3 signaling and promote lung adenocarcinoma progression. J Biochem Mol Toxicol 38: e23743, 2024.



Copyright © 2025 Watanabe et al. This work is licensed under a Creative Commons Attribution-NonCommercial-NoDerivatives 4.0 International (CC BY-NC-ND 4.0) License.